QUANTIFICATION OF WATER EXCHANGE BETWEEN INTRAVASCULAR AND EXTRAVASCULAR COMPARTMENTS USING INDEPENDENT COMPONENT ANALYSIS

Hatef Mehrabian[1,2], Anne L Martel[1,2], Johann Le Floc'h[1], Hany Soliman[1,3], Arjun Sahgal[1,4], and Greg J Stanisz[1,2]

[1]*Physical Sciences, Sunnybrook Research Institute, Toronto, Ontario, Canada,* [2]*Medical Biophysics, University of Toronto, Toronto, Ontario, Canada,* [3]*Odette Cancer Centre, Sunnybrook Health Sciences Centre, Toronto, Ontario, Canada,* [4]*Radiation Oncology, Sunnybrook Health Sciences Centre, Toronto, Ontario, Canada*

Introduction: Biomarkers based on quantitative measurements of tumor microvasculature can be used to assess tumor response to therapy. Conventional techniques, i.e. pharmacokinetic modeling[1], require measuring an arterial input function (AIF) which needs high temporal resolution MRI and ignores bolus dispersion and diffusion as it travels from the artery to the tumor. There is also high variability in model parameters due to inaccuracies in AIF measurement, and thus there is significant interest in developing novel biomarkers. We have previously developed an independent component analysis (ICA)-based algorithm to split DCE-MRI signal into its intravascular (IV) and extravascular (EV) components[2,3]. These signals are functions of contrast agent (CA) concentrations and water exchange rates between the two compartments. This study uses these IV and EV signals in a two-compartment relaxation model[4] to quantify water exchange rates and compartment sizes. We hypothesize these parameters are more sensitive to changes in tumor microenvironment and better reflect focal radiation treatment efficacy in patients.

Methods: Adaptive Kernel (AK)-ICA: Having X, a linear mixture of source signals S that are mixed with weight coefficients A ($X = AS$), ICA identifies the sources S and weights A, assuming these sources are spatially independent. We have previously developed an adaptive complex (AC)-ICA[2] algorithm that uses the complex-valued MRI signal and an adaptive cost function to split data into IV and EV components, assuming these compartments are spatially independent[4]. AK-ICA is an extension of this algorithm that uses the magnitude of MRI data and a kernel ($\varphi(S) \triangleq (1/\sqrt{2\pi})\exp(-s^2/2)$) to estimate the spatial distribution of each compartment at each iteration of ICA algorithm, and uses this estimated distribution in its ICA cost function.

Two-Compartment Relaxation Model: Each compartment (IV and EV) in a voxel contains a fraction of its total water content proportional to compartment size ($M_{0,IV}$, $M_{0,EV}$), such that $M_{0,IV} + M_{0,EV} = 1$. Water moves from IV to EV compartment with exchange rate k_{ie}, and from EV to IV compartment with k_{ei}, and at equilibrium we have $M_{0,IV}k_{ie} = M_{0,EV}k_{ei}$. Bloch equations of longitudinal magnetization, taking water movement between compartments into account, are[4,5]: $dM_{Z,IV}/dt = R_{1,IV}(M_{0,IV} - M_{Z,IV}) - k_{ie}M_{Z,IV} + k_{ei}M_{Z,EV}$ and $dM_{Z,EV}/dt = R_{1,EV}(M_{0,EV} - M_{Z,EV}) - k_{ei}M_{Z,EV} + k_{ie}M_{Z,IV}$ where $R_{1,IV}$, $R_{1,EV}$ are longitudinal relaxation rates. Solution of these coupled equations for SPGR sequence is (assuming negligible T_2 effect) $S = S_0\sin(\propto)\left(M_{0A}\frac{1-e^{-TR.R_{1A}}}{1-cos(\propto)\,e^{-TR.R_{1A}}} + M_{0B}\frac{1-e^{-TR.R_{1B}}}{1-cos(\propto)\,e^{-TR.R_{1B}}}\right)$ where

$$M_{0A} = \frac{1}{2} - \frac{1}{2}\frac{(R_{1,IV}-R_{1,EV})(M_{0,EV}-M_{0,IV})+k_{ie}+k_{ei}}{\sqrt{(R_{1,IV}-R_{1,EV}+k_{ie}-k_{ei})^2+4(k_{ie}k_{ei})}}, R_{1A} = \frac{R_{1,IV}+R_{1,EV}+k_{ie}+k_{ei}+\sqrt{(R_{1,IV}-R_{1,EV}+k_{ie}-k_{ei})^2+4(k_{ie}k_{ei})}}{2}, R_{1B} = \frac{R_{1,IV}+R_{1,EV}+k_{ie}+k_{ei}-\sqrt{(R_{1,IV}-R_{1,EV}+k_{ie}-k_{ei})^2+4(k_{ie}k_{ei})}}{2},$$

$M_{0B} = 1 - M_{0A}$, TR is repetition time, $\propto$ is flip angle, and S_0 is the equilibrium signal which cancels out if data is normalized to a pre-contrast image.

Solving for model parameters: CA concentration at each voxel (c) can be calculated through pre-contrast R_1 mapping and using SPGR signal equation. This concentration could be written in terms of its IV and EV fractions as $c = c_{IV}/M_{0,IV} + c_{EV}/M_{0,EV}$ where c_{IV} and c_{EV} are the IV and EV concentrations. Longitudinal relaxation rates of the compartments are: $R_{1,IV} = R_{10,IV} + r_1c_{IV}$ and $R_{1,EV} = R_{10,EV} + r_1c_{EV}$, where r_1 is the longitudinal relaxivity. Considering $R_{10,IV} = 1/1.65\ [s^{-1}]$ (at 3T, Hct $= 0.42$), the model has four independent parameters ($c_{IV}, R_{10,EV}, M_{0,IV}, k_{ie}$) for each voxel. In a DCE-MRI sequence three of these parameters are fixed for each voxel and c_{IV} is changing with time. The proposed ICA-based technique separates the IV and EV signals in DCE-MRI providing two equations for each voxel at each time point. Thus the model parameters could be calculated using a minimum of 3 time points.

Acquisition: 3 patients with metastatic brain tumors were scanned using a 3T Philips Achieva MRI scanner under IRB approved protocols. Each patient was imaged before and 6 days after focal radiotherapy. DCE-MRI was performed using 3D SPGR (TR/TE=4/2.02ms, FA=15°, FOV=25.6x25.6cm, Matrix 256x256x20, slice thickness 8mm). Variable flip angles (VFA) imaging was also performed with FA=3, 14, 130, 150° for B_1 and R_1 mapping.

Analysis: Pre-contrast R_1-map was used to convert MR signal of each voxel at each time point to its CA concentration. The AK-ICA was applied to each DCE-MRI dataset and the signal was split into its IV and EV compartments. Three time points (after CA arrival in tumor) were selected at random and their IV and EV MRI signals were normalized with respect to MR image at $t = 0$, and the exchange model equations were solved using these normalized signals and their voxel concentrations. To assess repeatability of the parameters calculation, model equations were solved for 10 different sets of 3 time points.

Results: Fig 1 shows a sample DCE-MR image and the R_1-map that was calculated using VFA, as well as mean and standard deviation maps (calculated using 10 different sets of 3 time points) of each parameter for one scan. Table 1 reports the mean and standard deviations of $M_{0,IV}$ and k_{ei} values for all 3 patients before and after treatment (over the tumor and a region of normal tissue).

Table 1 $M_{0,IV}$ and k_{ei} ranges for tumor/normal tissues for all 6 scans

		k_{ei-pre}	$k_{ei-post}$	$M_{0,IV-pre}$	$M_{0,IV-post}$
P1	N	0.002±0.005	0.08±0.06	0.02±0.02	0.12±0.08
	T	0.14±0.12	0.30±0.23	0.12±0.08	0.28±0.12
P2	N	0.014±0.035	0.016±0.04	0.03±0.04	0.03±0.06
	T	0.49±0.23	0.69±0.26	0.33±0.11	0.45±0.08
P3	N	0.12±0.08	0.014±0.013	0.15±0.07	0.08±0.06
	T	0.51±0.26	0.21±0.11	0.34±0.11	0.21±0.09

** pre: pre-treatment, post: post-treatment, N: normal tissue, T: tumor*

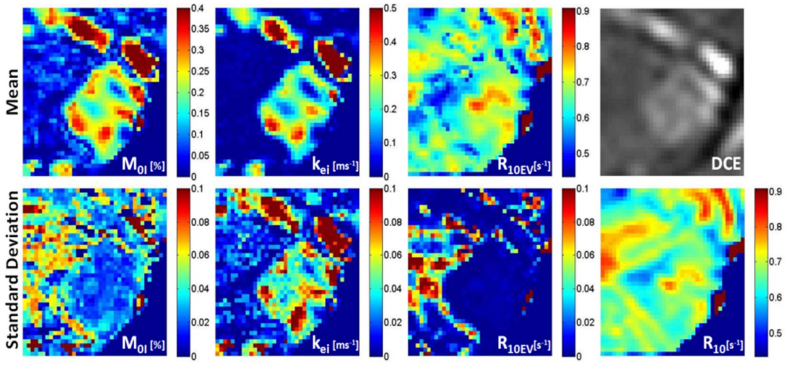

Fig 1. Mean and standard deviations of model parameters ($M_{0,IV}$, k_{ei}, $R_{10,EV}$) for one dataset as well as a sample DCE image and the pre-contrast R_1 calculated using VFA

Discussions and Conclusions: An important feature of the proposed model is that it does not require high temporal resolution DCE-MRI (although we used high temporal resolution data here). Also, since the IV signal is being measured locally at the tumor, it does not depend on the inaccuracies and discrepancies in AIF measurement. The results show the model is robust and $R_{10,EV}, M_{0,IV}$ have small variations. The exchange rate k_{ei} has large values particularly in the tumor (as expected), however its large variations are due to signal equations becoming insensitive to this parameter if: $k_{ei}(1 + M_{0,EV}/M_{0,IV}) \gg |R_{1,IV} - R_{1,EV}|$. These preliminary results show that k_{ei} is more sensitive to radiotherapy compared to K^{trans} in PK modeling (not reported here). Note that k_{ie} (k_{ei}) have high values and are fundamentally different from the K^{trans} (k_{ep}) values calculated in PK modeling which quantify exchange of CA that is a slower process.

References: [1] Tofts P, *et al.*, JMRI, **10** (3): 223-232, 1999. [2] Mehrabian H, *et al.*, IEEE Trans. Med. Imaging **32** (4): 699-710, 2013. [3] Mehrabian H, *et al.*, Eur Radiol., **22** (8): 1735-1747, 2012. [4] Bailey C, *et al.*, MRM **71** (5): 1874-87, 2014. [5] McConnel HM, *et al.*, J Chem Phys **28** (3): 430-431, 1958.